We are IntechOpen, the world's leading publisher of Open Access books Built by scientists, for scientists

4,800
Open access books available

122,000
International authors and editors

135M
Downloads

Our authors are among the

154
Countries delivered to

TOP 1%
most cited scientists

12.2%
Contributors from top 500 universities

CLARIVATE ANALYTICS BOOK CITATION INDEX INDEXED

WEB OF SCIENCE™

Selection of our books indexed in the Book Citation Index in Web of Science™ Core Collection (BKCI)

Interested in publishing with us?
Contact book.department@intechopen.com

Numbers displayed above are based on latest data collected.
For more information visit www.intechopen.com

2

EMG Analysis Methods on Robotic Gait Machines

Christopher Tomelleri[1], Andreas Waldner[1] and Stefan Hesse[2]
[1]*Privatklinik Villa Melitta*
[2]*Medical Park Berlin Humboldtmühle*
[1]*Italy*
[2]*Germany*

1. Introduction

Gait impairment is one of the consequences of events like stroke, traumatic brain injury, spinal cord injury or neurodegenerative diseases like Multiple Sclerosis or Parkinsons' Disease. The restoration and improvement of walking functions is one of the primary concerns of the rehabilitation of neurological Patients. To achieve this goal, a task specific repetitive training seems the most promising strategy (Jorgensen et al., 1995).
Conventional physiotherapy stresses out the reduction of an elevated muscle tone and the practice of gait preparatory tasks while sitting or standing. Accordingly, the number of steps practised rarely exceeds 50 to 80 steps during one therapy session (Hesse et al., 1995).
To increase the number of steps during therapy, the treadmill training with partial body weight support was a first step. Over the last years, there has been a growing support for the use of manual assisted treadmill training in neurorehabilitation programs. Studies showed that individuals who receive body weight supported treadmill training following stroke, traumatic brain injury and spinal cord injury improve their muscle activity during locomotion and gait symmetry. The main limitation with manual assisted body weight supported treadmill therapy is that a training session relies on several physical therapists to assist the patients' leg and hip movements through the gait cycle by hand. This results in short training sessions because of the physical effort required by the therapists and limits the potential of the treatment for the required training intensity may not be reached (Barbeu & Visintin 2003).
Robotic Gait Machines were developed to bypass these limiting factors. The gait machines move the legs of the patients through specified patterns. This is made either by applying an exoskeleton or an end-effector principle. The exoskeleton devices known so far are the Lokomat (Colombo et al., 2000), the LOPES (Veneman et al. 2007), the AutoAmbulator (Healthsouth Corporation, 2004) and the Sarà (MPD Costruzioni Meccaniche, 2010). Typical end-effector devices are the GangTrainer GT I (Hesse & Uhlenbrock, 2000), the LokoHelp (Freivogel et al., 2008), the Hapic Walker (Schmidt et al., 2005), the 6 Degrees of Freedom Gait Robot (Yoon et al., 2010) and the G-EO Systems (Hesse et al., 2010).
The exoskeleton is equipped with programmable drives or passive elements which flex the knees and hips during the swing phase. With the other principle the feet are placed on foot

plates, whose trajectories simulate the stance and swing phases. The potential risk of Robotic Gait Machines is the introduction of a non physiological gait pattern due the limited degrees of freedom controlled by the machines.

An understanding of the biomechanical interaction between Robotic Gait Machines and patients during locomotor training on the device is relevant to ensure correct interaction forces applied on the patients' joints and the correct activation of their muscles. Typically a gait analysis system is applied on patients or on healthy subjects while walking on the Robotic Gait Machine.

The EMG Analysis on a gait robot aims to prove the correctness of the induced muscle activation while practising on the machines. If the selected muscles are activated in a correct fashion, any concerns about an incorrect training pattern would be inconsistent. The purpose of the present chapter is to introduce, explain and compare the methods of different EMG analyses carried out on different robotic gait machines, i.e. to present the gait robots, the subject pool, the data acquisition and the signal processing strategies. This is made by explaining in detail the choices and techniques represented in the respective Methods section of the studies considered.

2. EMG analysis methods on robotic gait machines

EMG Analyses have been made so far on three different gait robots: the Lokomat (Hidler & Wall), the Haptic Walker (Hussein, 2009) and the G-EO Systems (Hesse et al., 2010). All three studies addressed the essential question of a match between muscle activation patterns of the subjects under test during training on the Robotic Gait Machine and during free walking.

The Lokomat robotic gait orthosis consists of a treadmill, a body weight support system and two light weight robotic actuators to attach to the subjects' legs. The robotic actuators are fully programmable and control the flexion and the extension of the knee and the hip. The actuators are synchronized with the treadmill for setting the correct speed while walking. The movement of the ankle is not controlled; a spring provides for dorsiflexion and avoids the paretic foot to stumble on the treadmill. The Lokomat also controls the speed at which the patient ambulates and the amount of assistance the system provides to the patient.

The HapticWalker is an end-effector robot, designed following the programmable footplate concept. Each of the two foot plates consists of a hybrid serial-parallel robot. The patients' feet are fixed on the foot plates, which move the patients' feet along the natural movement of walking. For the end-effector principle if the last segment of a kinematic chain is moved correctly, all segments and joints in the kinematic chain are moved correctly. It follows that by controlling and moving the foot correctly, the knee and the hip are also moved correctly by the gait robot.

The G-EO Systems follows the end effector principle as well. The patient stands on two foot plates, connected each by a crank arm to two moving units. The G-EO Systems is more compact in the design than the Haptic Walker as it was designed to be a clinically feasible end-effector robot.

The devices differ in their design strategy. The Lokomat follows the exoskeleton principle; the Haptic Walker and the G-EO Systems are end effector based devices. Figure 1 shows the three devices.

Fig. 1. The Lokomat, the Haptic Walker and the G-EO Systems.

2.1 Test protocol

The Lokomat study enrolled a total of seven healthy subjects with no known neurological injuries or gait disorders, the Haptic Walker study a total of nine healthy subjects. The G-EO Systems Study was conducted on six ambulatory stroke patients.

The Lokomat and the Haptic Walker provided gait velocities suitable to a gait analysis on healthy subjects. It was possible to analyze the gait with no restrictions to gait velocity and cadence of the subjects under test. A restriction of walking speed would have prolonged the duration of muscle activation or altered the timing in the muscle activation patterns. The aim of both studies was to show a match between EMG patterns of real walking and robotic walking.

Having an analysis on the G-EO Systems on healthy subjects would have been senseless, as the trajectories of the Haptic Walker and the G-EO Systems were quite the same. The motion tracking of healthy subjects was made with the same active marker system, but on a different population (Hesse et al., 2010; Schmidt et al. 2005). The aim for the G-EO Systems was not to replicate the results of the Haptic Walker study, which clearly proved a physiological muscle activation on the end-effector robotic gait machine, but to extend these results to another study population.

Furthermore the G-EO Systems was designed for treating gait impaired patients and did not provide gait velocities suitable for an analysis on healthy subjects. A gait analysis on subjects whose own walking speed would have been superior to the one provided by the machine would have altered the EMG patterns. The Authors were looking for subjects able to walk freely on speeds comparable to the maximum speed provided by the G-EO Systems. This was the reason of having the analysis made on ambulatory stroke patients.

2.2 Data acquisition

The Lokomat Subjects walked first on the treadmill without the Lokomat and then with the Lokomat orthoses. The Lokomat linkages were adjusted to the leg lengths of each subject, so that the hip and knee joints of the Lokomat were aligned with those of the subject. During

both Lokomat and treadmill walking, surface EMGs were recorded differentially from the gastrocnemius, tibialis anterior, hamstrings, rectus femoris, adductor longus, vastus lateralis, and gluteus medius and maximus muscles using a 8 channel EMG system.

The gastrocnemius is involved in all standing, walking, running and jumping activities. Its function is the plantar flexion of the foot at the ankle joint and the flexion of the leg at the knee joint.

The tibialis anterior is responsible for dorsiflexing and inverting the foot. The tibialis anterior muscle also allows the ankle to be inverted providing horizontal movement. The muscle stabilizes the ankle as the foot hits the ground during the contact phase of walking through eccentric contraction and acts later to pull the foot clear of the ground during the swing phase by concentric contraction.

The hamstring muscles include three posterior thigh muscles: the semitendinosus, the semimembranosus and the biceps femoris. They act upon the hip and the knee joints. The semitendinosus muscle and the semimembranosus muscle extend the hip when the trunk is fixed. They also flex the knee and provide for medial rotation of the lower leg when the knee is bent. The long head of the biceps femoris extends the hip when starting to walk. Short and long heads of the biceps femoris flex the knee and provide for lateral rotation of the lower leg when the knee is bent.

The rectus femoris muscle is one of the four quadriceps muscles and is situated in the middle of the front of the thigh. The rectus femoris is one of the muscles in the quadriceps involved in the flexion of the hip. By crossing the pelvic femoral joint it can act as a lever to flex the leg at the hip.

The adductor longus is a muscle located in the thigh. The main function is to adduct and laterally rotate the femur. The adductor lies ventrally on the adductor magnus and near the femur.

The vastus lateralis muscle is on the lateral side of the femur and is the largest of the quadriceps muscles. Like all quadriceps muscle its function is to act as an extensor of the knee.

The gluteus medius muscle is one of the three gluteal muscles. With straightened leg the gluteus medius function is to abduct the thigh. During gait the gluteus medius principally supports the body on one leg to prevent the pelvis from dropping to the opposite side. With the hip flexed the gluteus medius rotates the thigh externally. With the hip extended, the gluteus medius rotates the thigh internally.

The gluteus maximus muscle is another gluteal muscle, the largest and most superficial of the three gluteal muscles. Considering the pelvis as fixed the gluteus maximus extends the femur.

Only one leg was instrumented with EMG electrodes since none of the subjects had any gait disorders and walked symmetrically. The EMG data was collected for 60 seconds.

The EMG Signals of the Haptic Walker Subjects EMG were acquired during free walking and during walking on the HapticWalker. For robot assisted walking the same step length as calculated from free walking was used. At least 5 full stride cycles were taken for each trial. The surface EMGs were recorded from the tibialis anterior, gastrocnemius, rectus femoris, biceps femoris, vastus medialis, vastus lateralis, gluteus medius and erector spinae muscles using a 8 channel EMG system.

The biceps femoris belongs to the hamstring muscles and is responsible for knee flexion. The long head is also involved in hip extension. When the knee is semi-flexed, the biceps femoris rotates the leg slightly outward.

The vasus medialis translates the patella medially and provides control of the knee extension together with the vastus lateralis. The vastus medialis is medially located in the quadriceps muscle group.
The Erector spinae is a muscle group. It extends throughout the lumbar, thoracic and cervical regions, and lies in the groove to the side of the vertebral column.
Only one side was instrumented with EMG electrodes since none of the subjects had any gait disorders and walked symmetrically.
The subjects on the G-EO Systems were analysed while walking on the floor at self selected speed and during simulated floor walking on the machine at comparable speed and cadence. The EMG activity was measured on seven lower limb muscles: tibialis anterior, gastrocnemius, vastus medialis, vastus lateralis, rectus femoris, biceps femoris, and gluteus medius of the affected side. The non affected side was not of interest for the purposes of the study. The muscles under analysis were the same as for the Haptic Walker, but did not include the erector spinae. The activation pattern for this muscle group showed to be too weak on hemiparetic patients. The assessment consisted of a 30 seconds long recording of the electromyographic activity during real and simulated floor walking. The subjects were first asked to walk on the floor for at least 30 seconds at a self selected pace. Gait velocity, step length and cadence of free walking were replicated on the gait robot.

2.3 Signal processing

Signal Processing was made for all three studies according to Fourier Analysis (Oppenheim et al., 1996). The bandwidth of the EMG signal was considered as limited, i.e. the Fourier Transform of the EMG Signal is zero outside of a finite band of frequencies. The Fourier transform is a mathematical operation that decomposes a signal into its constituent frequencies. The Fourier Transform for a continuous time signal is given by

$$X(f) = \int_{-\infty}^{+\infty} x(t)\, e^{-j2\pi ft}\, dt \tag{1}$$

Every continuous time signal may be also represented by his frequency content. A signal with infinite bandwidth can be lowpass filtered to a finite bandwidth signal. In the time domain this operation would consist in a convolution operation between the infinite band signal x(t) and the function in the time domain of the lowpass filter h(t), resulting in the finite band signal y(t) given by

$$y(t) = x(t) * h(t) \tag{2}$$

$$y(t) = \int_{-\infty}^{+\infty} x(\tau)\, h(t-\tau)\, d\tau \tag{3}$$

The convolution in the time domain between x(t) and h(t) becomes a multiplication operation in the frequency domain between X(f) and H(f) , due to duality proprieties of the Fourier Transform. The Fourier Transform Y(f) of the limited band signal y(t) is given by

$$Y(f) = X(f)\, H(f) \tag{4}$$

Mind that lowpass filtering a infinite band signal results in a loss of information or a lossy compression. The cut-off frequency of the lowpass filter H(f) should therefore be chosen adequately. Figure 2 shows an infinite band signal, an ideal lowpass filter and a finite band signal as the product in the frequency domain of the infinite band signal and the lowpass filter.

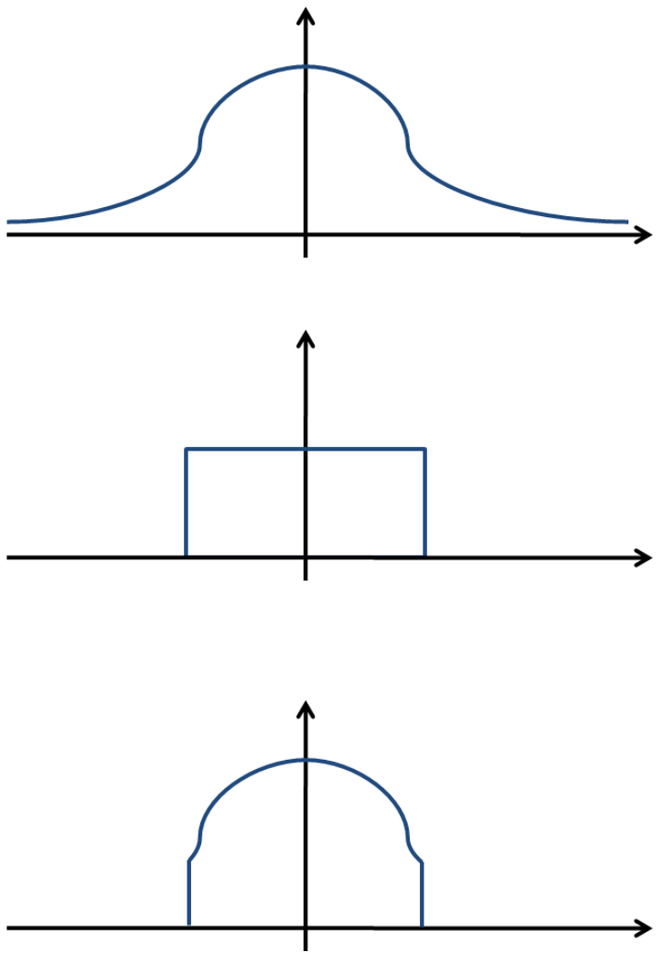

Fig. 2. Infinite band signal, ideal lowpass filter and finite band signal as product in frequency of the infinite band signal and the lowpass filter.

If the samples of the signal are taken sufficiently close together in correspondence to the highest frequency of the signal, then the samples uniquely specify the signal. The correct frequency for sampling a limited band signal is given by the Sampling Theorem which states:

Let x(t) be a band-limited signal with X(f) = 0 for | f | > f_M. If the Sampling Frequency f_S > f_M, Then x(t) is uniquely determined by its samples x(nT), n = 0, ±1, ±2,..., where T = 1/f_S. The signal can be reconstructed by an ideal lowpass filter with gain T and cut-off frequency f_C , where f_M > f_C > f_S - f_M.

The usual way of representing a finite band signal in regular intervals is the multiplication of the continuous-time signal x(t) and a periodic impulse train p(t). This is known as impulse train sampling. In the time domain the signal $x_p(t)$ results from

$$x_p(t) = x(t)\, p(t) \tag{5}$$

where

$$p(t) = \sum_{n=-\infty}^{+\infty} \delta(t - nT) \tag{6}$$

Multiplying x(t) by a unitary impulse train samples the values of the signal at the points at which the impulses were located. The signal $x_p(t)$ therefore is an impulse train with the amplitudes of the impulses equal to the samples of x(t) at intervals spaced by T; that is

$$x_p(t) = \sum_{n=-\infty}^{+\infty} x(nT)\,\delta(t - nT) \tag{7}$$

Again by duality proprieties between the time domain and the frequency domain, the multiplication in the time domain becomes a convolution in the frequency domain

$$X_p(f) = \frac{1}{2\pi} \int_{-\infty}^{+\infty} X(\varphi) P(f - \varphi) d\varphi \tag{8}$$

with

$$P(f) = \frac{1}{T} \sum_{k=-\infty}^{+\infty} \delta(f - f_s) \tag{9}$$

The convolution with an impulse $\delta(f_0)$ shifts a signal X(f)

$$X(f) * \delta(f - f_0) = X_p(f - f_0) \tag{10}$$

it follows

$$X_p(f) = \frac{1}{2\pi T} \sum_{k=-\infty}^{+\infty} X(f - f_s) \tag{11}$$

It means that $X_P(f)$ is a periodic function of f consisting of a superposition of shifted replicas of X(f) scaled by $1/2\pi T$. If the sampling frequency is chosen according to the Sampling Theorem, there is no overlap between $X_P(f)$ and its replicas. The signal x(t) can be reconstructed correctly using the lowpass filter suggested by the Sampling Theorem.

If the signal is not sampled according to the Sampling Theorem, there would be an overlap between X(f) and its replicas. The overlap results in the higher frequency components in the band of the signal summing and introducing distortion in $X_P(f)$. The signal x(t) could not be reconstructed correctly any more, this phenomenon is referred to as Aliasing. For finite band signals the Sampling Frequency has to be chosen correctly, for infinite band signals there has to be a lowpass filtering prior to sampling. As the aim of this filtering is to avoid the Aliasing Phenomenon, it is also called Anti-Aliasing or Anti-Alias Filtering.

Figure 3 shows the replicas of an infinite band signal overlapping, the result of overlapping and the same signal filtered by an ideal lowpass filter to prevent overlapping.

It is important to notice that the pre-filtering has to be an analogical lowpass filtering and has to happen before sampling. It is good practice to pre-filter finite bandwidth signals as well. Although the band of this kind of signals is finite, there could be spurious components outside the signal band, i.e. disturbances at higher frequencies which superimpose to the signal to sample. Sampling without pre-filtering would sample the disturbances too. If the Sampling Frequency is chosen correctly for the signal to sample, but does not match the Sampling Theorem for the high frequency disturbances, the replicas of the disturbances would overlap on the signal introducing distortion. Pre-filtering with a cut-off frequency equal or below the Sampling Frequency would eliminate disturbances to the signal from the beginning.

Figure 4 shows a finite band signal and a disturbance, the sampled signal with the disturbance overlapping on the signal and the signal filtered prior to sampling by an ideal lowpass filter to prevent disturbances.

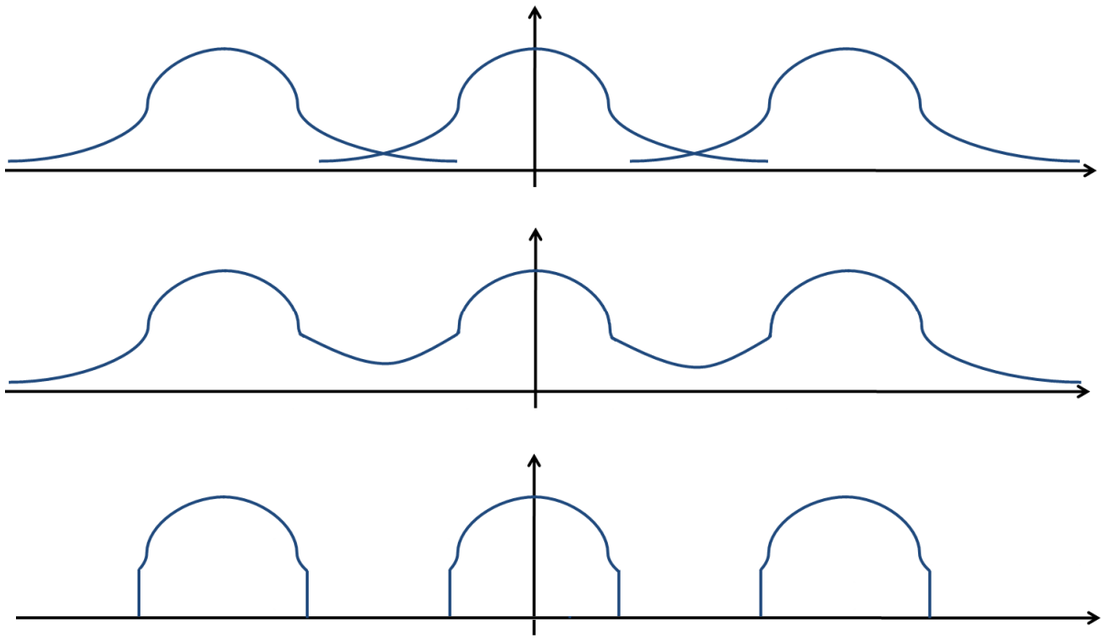

Fig. 3. Aliasing phenomenon resulting in overlapping replicas summing up and result of an Anti-Alias Filtering.

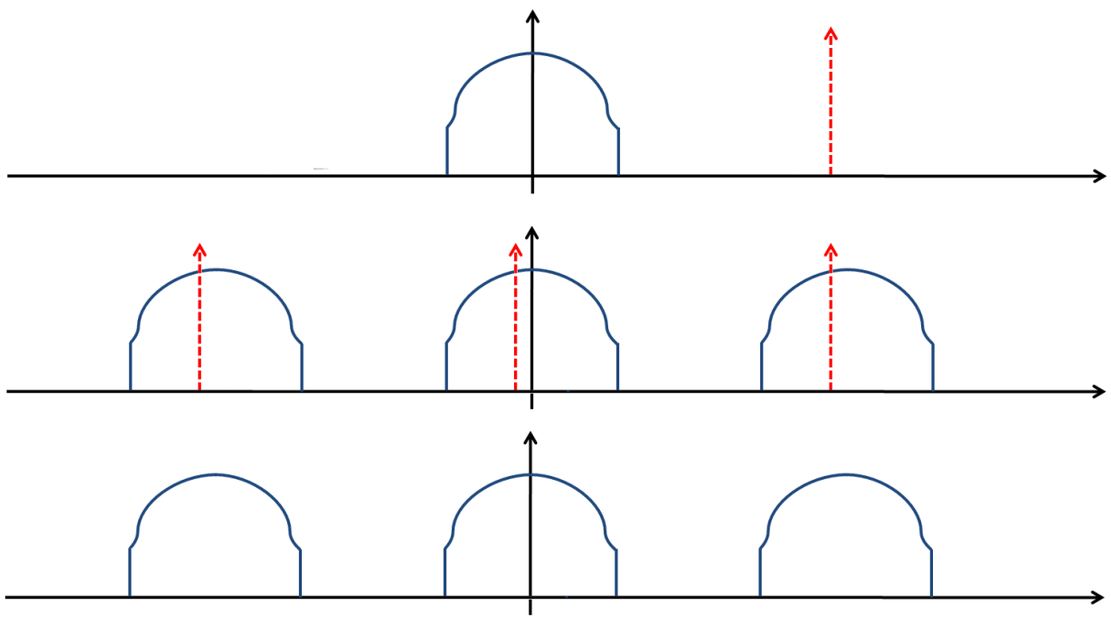

Fig. 4. High frequency disturbances on a finite band signal and result of ideal lowpass filtering prior to sampling.

After sampling all signal processing strategies would be digital. Digital lowpass filtering after sampling would not be a Anti-Alias Filtering. Mind that the signal would be already aliased and that lowpass filtering with a cut-off frequency equal to the Sampling Frequency would be useless. Digital filtering can improve proprieties of the correctly sampled signal as it can provide for smoothing or compression of the signal itself, but it can never provide for Anti-Aliasing.

The EMG signal is not a finite band signal, although the information content above 500 Hz is negligible. A good choice of the cut-off frequency of an ideal lowpass filter for pre-filtering purposes therefore is 500 Hz, resulting in a typical Sampling Frequency of 1000 Hz, twice the cut-off frequency of pre-filtering. On the Lokomat , on the Haptic Walker and on the G-EO Systems the EMG signals were lowpass filtered at 500 Hz prior to sampling at 1000 Hz to avoid the aliasing phenomenon by the EMG analysis system. On the G-EO Systems the sampled data were further filtered by a Finite Impulse Response (FIR) filter of first order lowpass filter with Z-Transform

$$H(z) = \frac{1}{2}\frac{1z}{1+z} \tag{12}$$

The filter was intended for additional smoothing of the raw EMG signal for the following signal processing without affecting the useful information content in the signal band.

Additional signal filtering on the Haptic Walker was provided by a full wave rectification, followed by a highpass filtering to suppress measurement artifacts.

A full wave rectification converts the whole of the input signal to a signal of constant polarity at its output. The raw EMG signal has random variations between negative and positive peaks. By full wave rectification all negative amplitudes are converted to positive amplitudes, i.e. for a the raw EMG x(t) the full wave rectified output y(t) would be

$$y(t) = |x(t)| \tag{13}$$

The negative spikes are moved to positive values reflected on the baseline. Besides easier reading the main effect is that standard amplitude parameters like mean and area can be applied to the signal. The non rectified raw EMG has a mean value and area under signal of zero.

High-pass filtering of EMG signals is used to remove possible movement artifacts comprised in a low frequency range. Typical highpass filters for EMG signals start at a frequency between 10 and 20Hz.

2.4 Step determination and envelope calculation

The single steps were determined by the trigger signal provided by the foot switches of the EMG analysis system on the Lokomat and on the G-EO Systems.

For the Haptic Walker the trigger signal for determination of the single was provided by the gait robot itself. The reason for this choice was due to the end-effector principle. On the end-effector robots the feet have continuous contact to the footplate, i.e. the leg is supported by the robot not only during the stance phase but also during the swing phase. This would create an offset on the foot switches of the EMG analysis system for there would be easily some residual pressure on the foot switch. This would make it difficult for the analysis system to distinguish between the stance and the swing phase. Taking the data of the trigger signal directly from the gait robot bypassed the problem, furthermore it provided for stride

intervals of exactly the same duration between all the triggering peaks within the trigger signal.

Although the EMG analysis system used for the G-EO Systems was the same as for the Haptic Walker, the trigger signal was taken from the foot switches. The safety binding on the G-EO System allowed for more flexibility than the one of the Haptic Walker, resulting in less offset pressure on the foot switches. A further observation showed that the hemiparetic patients under test did not load the affected leg in the swing phase but loaded the non affected leg as much as possible. Under these considerations the trigger signal provided by the footswitches showed to be suitable for an analysis on an end-effector robot too.

After triggering the EMG signal the patterns for each stride had to be normalized in time. This had to be done in the case of the trigger signals taken by the foot switches, but not if the trigger signal was taken from the machine. The timing of the trigger peaks and the duration of the trigger intervals taken by the footswitches differed in a few milliseconds, resulting in a different number of samples associated to the single strides. On the Lokomat this was due to the fact that the ankle and the heel were not controlled by the gait robot, and on the G-EO Systems due to intra-subject variability of the strides made by the hemiparetic patients walking on the gait machine, although the machine provided for perfectly symmetrical walking.

Normalization was achieved by upsampling the single strides of the EMG signal and by resampling the upsampled strides to the same number of samples for each stride. Upsampling was made with the help of a cubic spline (Giakas & Baltzopoulos, 1997). A cubic spline was constructed of piecewise third-order polynomials which passed through a set of m control points. Weights were associated to the points to be connected by the third order polynomials. These coefficients bent the polynomials to pass through each of the data points without any erratic behavior or breaks in continuity. Considering a function of the form:

$$S(x) = \begin{cases} s_1(x) & if \quad x_1 \le x < x_2 \\ s_2(x) & if \quad x_2 \le x < x_3 \\ & \vdots \\ s_{n-1}(x) & if \quad x_{n-1} \le x < x_n \end{cases} \tag{14}$$

Where s_i was the third order polynomial defined as

$$s_i(x) = a_i\,(x - x_i)^3 + b_i\,(x - x_i)^2 + c_i\,(x - x_i) + d_i \tag{15}$$

for i = 1,..,n-1. The first and the second derivative of these n-1 equations were

$$s'_i(x) = 3a_i\,(x - x_i)^2 + 2b_i\,(x - x_i) + c_i \tag{16}$$

$$s''_i(x) = 6a_i\,(x - x_i) + 2b_i \tag{17}$$

for i = 1,..,n-1. The cubic spline needed to conform to the following:

1. The piecewise function S(x) had to interpolate all data points.
2. *S(x)* had to be continuous on the interval [x_1 , x_n]
3. *S′(x)* had to be continuous on the interval [x_1 , x_n]
4. *S′′(x)* had to be continuous on the interval [x_1 , x_n]

S(x) had to interpolate all of the samples, for i = 1,…, n-1

$$S(x_i) = y_i \tag{18}$$

Since $S(x_i) = y_i$ for all x_i in the closed interval $[x_i, x_{i+1}]$

$$y_i = s_i(x_i) \tag{19}$$

By substitution of (15) in (19)

$$y_i = d_i \tag{20}$$

The curve S(x) must be continuous in its entire interval, the subfunctions had to join at the samples

$$s_i(x_i) = s_{i-1}(x_i) \tag{21}$$

For i = 1,…,n. Letting $h = x_i - x_{i-1}$, the subfunction $s_{i-1}(x_i)$ was defined as

$$s_{i-1}(x_i) = a_{i-1}h^3 + b_{i-1}h^2 + c_{i-1}h + d_{i-1} \tag{22}$$

$$d_i = a_{i-1}h^3 + b_{i-1}h^2 + c_{i-1}h + d_{i-1} \tag{23}$$

The curve would only have been smooth across its interval only if the derivates were equal at the samples; that is

$$s_i'(x_i) = s'_{i-1}(x_i) \tag{24}$$

Solving for $s'_i(x_i)$ and $s'_{i-1}(x_i)$, considering again $h = x_i - x_{i-1}$

$$s'_i(x_i) = c_i \tag{25}$$

$$s'_{i-1}(x_i) = 3a_{i-1}h^2 + 2b_{i-1}h + c_{i-1} \tag{26}$$

By substitution of equation (25) in equation (26) c_i could be expressed for i = 2,…, n-1 as

$$c_i = 3a_{i-1}h^2 + 2b_{i-1}h + c_{i-1} \tag{27}$$

Solving equation (17) for $x = x_i$

$$s''_i(x_i) = 2b_i \tag{28}$$

For i = 2,…n-2.
Since $s''_i(x)$ had to be continuous across the interval, $s''_i(x_i) = s''_{i+1}(x_i)$ for i = 1,…,n-1. Considering this and equation (28) with $h = x_{i+1} - x_i$

$$s''_i(x_{i+1}) = 6a_i h + 2b_i \tag{29}$$

$$s''_{i+1}(x_{i+1}) = 2b_{i+1} \tag{30}$$

$$2b_{i+1} = 6a_i h + 2b_i \tag{31}$$

For easier notation $s''_i(x)$ was substituted by M_i. Expressing the equations (31) and (28) in terms of M_i and y_i resulted in the determination of the weights of the cubic spline a_i, b_i, c_i and d_i.

$$2b_{i+1} = 6a_i\,h + 2b_i \tag{31}$$

$$6a_i\,h = 2b_{i+1} - 2b_i$$

$$a_i = \frac{2b_{i+1} - 2b_i}{6h}$$

$$a_i = \frac{M_{i+1} - M_i}{6h} \tag{32}$$

$$s''_i(x_i) = 2b_i \tag{28}$$

$$M_i = 2b_i$$

$$b_i = \frac{M_i}{2} \tag{33}$$

$$d_i = a_{i-1}h^3 + b_{i-1}\,h^2 + c_{i-1}h + d_{i-1} \tag{23}$$

$$d_{i+1} = a_i h^3 + b_i\,h^2 + c_i h + d_i$$

$$c_i h = -a_i h^3 - b_i\,h^2 - d_i + d_{i+1}$$

$$c_i = \frac{-a_i h^3 - b_i\,h^2 - d_i + d_{i+1}}{h}$$

$$c_i = -a_i h^2 - b_i\,h + \frac{-d_i + d_{i+1}}{h}$$

$$c_i = \frac{y_{i+1} - y_i}{h} - \frac{M_{i+1} - M_i}{6h}\,h^2 - \frac{M_i}{2}\,h$$

$$c_i = \frac{y_{i+1} - y_i}{h} - \left(\frac{M_{i+1} + 2M_i}{6}\right)h \tag{34}$$

$$y_i = d_i \tag{20}$$

$$d_i = y_i \tag{35}$$

After upsampling and resampling all strides were of the same number of samples, but the information about the duration of the strides got lost. Normalization expressed the samples in relation to the gait cycle: A whole stride is considered as 100% of the gait cycle, every sample is put in relation to this gait cycle percentage. The gait cycle starts with the initial contact and ends at the subsequent initial contact. The gait cycle percentages ranging from 0% to 60% were considered as stance phase, the percentages from 60% to 100% were considered as swing phase.

Upsampling was not necessary for the Haptic Walker. The stride duration was exactly the same for all strides of the measurement, due to the trigger signal taken from the device. The EMG data were just normalized in relation to the gait cycle.

The envelope of the strides was determined with root mean square algorithms (Simons & Yang, 1991). The root mean square of the n samples a signal x_i, i = 1,…,n, is given by

$$RMS = \sqrt{\frac{\sum_{i=1}^{n} x_i}{n}} \tag{36}$$

For the Lokomat and the G-EO Systems the root mean square algorithm consisted in a 50-point root mean square, 150-point root mean square respectively. A k-point root mean square is defined as:

$$x_i = \sqrt{\frac{\sum_{l=i}^{i+k-1} x_l}{k}} \tag{37}$$

The sample x_i is determined not as the whole root mean square of the sampled signal, but as the root mean square of the i^{th} sample and its following k-1 samples. This technique can be compared with a moving average filtering. Considering the signal x_i, with i = 1,…,n, for all samples of x_i where n-k+2 < i < n, the signal has to be replicated considering the samples from 1 to k-1 as the samples n+1 to n+k-1. The more samples are considered for the root mean square, the smoother the signal gets. For the Lokomat study the value chosen for k was 50, for the G-EO Systems 150. The final result of signal processing of the EMG signal in the Lokomat study therefore was more rippled than in the G-EO Systems study.

On the Haptic Walker the root mean square algorithm was based on a lowpass Bessel filer. A lowpass Bessel filter has a maximally flat group delay. Group delay is a measure of the time delay of the amplitude envelopes of the various sinusoidal components of a signal as a function of the frequency of each component. Analog Bessel filters are characterized by almost constant group delay across their passband, thus preserving the wave shape of signals filtered. The Laplace transform of the transfer function of a Bessel lowpass filter is expressed as (Barozzi, 2005):

$$H(s) = \frac{\vartheta(0)}{\vartheta(S/\omega_0)} \tag{38}$$

where ω_0 is a pulsation chosen to give the desired cut-off frequency. The Bessel lowpass filter therefore has a low-frequency group delay of 1 / ω_0. Pulsation and frequency are closely related as:

$$\omega = 2\pi f \tag{39}$$

θ(s) is a reverse Bessel polynomial described by

$$\vartheta(s) = \sum_{k=0}^{n} \frac{(2n-k)!}{(n-k)!k!} \frac{s^k}{2^{n-k}} \tag{40}$$

with s expressed as a complex number s = σ + jω.

The final mean EMG patterns generated for the gait cycle of all three studies were computed for each subject by averaging all the individual stride cycles of the subject. If the EMG signal consists of k single strides, contained in the signal s(i) with i = 1,...k*n, the average signal samples S(i) with i = 1,…,n of k strides is given by

$$S(i) = \frac{1}{k} \sum_{l=1}^{k} s(l * i) \tag{41}$$

3. Conclusion

The present chapter highlighted the differences in the protocols and the different techniques in EMG signal processing of three studies on robotic gait machines. The results of the

studies are not compared or discussed in this chapter, as the description of the methods showed differences which highlight how difficult a comparison would be.
The Lokomat study and the G-EO systems study had a similar signal processing strategy and a similar acquisition protocol. The G-EO Systems study in fact was inspired by the methods of the Lokomat study, but did not include healthy subjects, for the gait velocity provided by the G-EO Systems was too slow and a EMG signal analysis was already published for healthy subjects for the programmable foot plate concept taking in consideration the Haptic Walker. A comparison between the EMG signals of healthy subjects and stroke patients is difficult given the fact the muscle activation patterns of hemiparetic subjects differ considerably from healthy muscle activation patterns. Furthermore the individual patterns of hemiparetic patients vary considerably.
The Lokomat study and the Haptic Walker study both involved healthy subjects, but differed in the acquisition protocol and in the signal processing too. The Haptic Walker considered mostly just five strides during data acquisition and based its signal processing on different techniques, as explained in the previous sections.
The direct comparison between the Methods of the G-EO Systems study and the Haptic Walker study showed the use of the same design principle, the same data acquisition system, but different signal processing. The G-EO Systems study can be considered as an extension of the findings and the aims of the Haptic Walker study, but carried out with the Methods of the Lokomat study.
If looking for a comparison, the only way would be an analysis on these devices with the same protocol on a cluster of comparable patients with the same gait impairment. The acquired data should than be processed in the same way for the whole cluster of patients.

4. Acknowledgment

G-EO Systems was supported by a grant of the "Amt für Innovation, Landesregierung Südtirol", Italy. Scientific publication activities are also supported by the Landesregierung Südtirol, Italy and a grant of the Bundesministerium für Bildung und Forschung (BioFuture) of the German Government.

5. References

Barbeau, H. & Visintin, M. (2003). Optimal outcomes obtained with body-weight support combined with treadmill training in stroke subjects. *Archives of Physical Medicine and Rehabilitation,*Vol. 84, No. 10, (October 2003), pp. 1458-1465, ISSN 0003-9993

Barozzi G. (2005). *Matematica per ingegneria dell' informazione*, Zanichelli, ISBN 978-88-08-12546-0, Bologna, Italy

Colombo, G.; Joerg, M.; Schreier, R.; Dietz, V. (2000). Treadmill training of paraplegic patients using a robotic orthosis. *Journal of Rehabilitation Research and Development*, Vol. 37, No. 6, (November-December 2000) pp. 693-700, ISSN 0748-7711

Freivogel, S.; Mehrholz, J.; Husak-Sotomayor; T.; Schmalohr D. (2008). Gait training with the newly developed 'LokoHelp'-system is feasible for nonambulatory patients after

stroke, spinal cord and brain injury. A feasibility study. *Brain Injury*, Vol. 22, No. 7, (July 2008), pp. 625-632, ISSN 1362-301X

Giakas, G. & Baltzopoulos V. (1997) A comparison of automatic filtering techniques applied to biomechanical walking data, *Journal of Biomechanics*, Vol. 30, No. 8, (August 1997), pp. 847–850, ISSN 0021-9290

Healthsouth Corporation. (2004). Powered gait orthosis and method of utilizing same. US Patent US2004/0143198

Hesse, S.; Bertelt, C.; Jahnke, M.; Schaffrin, A.; Baake, P.; Malezic, M.; Mauritz, K. (1995). Treadmill training with partial body weight support as compared to physiotherapy in non-ambulatory hemiparetic patients. *Stroke,* Vol. 26, pp. 976-981, ISSN 0039-2499

Hesse, S. & Uhlenbrock, D. (2000). A mechanized gait trainer for restoration of gait, *Journal of Rehabilitation Research and Development*, vol. 37, no. 6, (September 2000), pp. 701–708, ISSN 0003-9993

Hesse, S.; Waldner, A.; Tomelleri, C. Innovative gait robot for the repetitive practice of floor walking and stair climbing up and down in stroke patients. (2010) *Journal of NeuroEngineering and Rehabilitation*, Vol. 7, No. 30, (June 2010) pp. 1-10, ISSN 1743-0003

Hidler, J. & Wall, A. (2005). Alterations in muscle activation patterns during robotic-assisted walking. *Clinical Biomechanics* Vol. 20, (February 2005), pp. 184–193, ISSN 0268-0033

Hussein, S.; Schmidt, H.; Krüger, J. (2009) Adaptive control of an endeffector based electromechanical gait rehabilitation device, *Proceedings of the IEEE 11th International Conference on Rehabilitation Robotics, ICORR 2009*, pp. 366-371, ISSN 1945-7898, Kyoto, Japan, 23-26 June, 2009.

Jorgensen, H.; Nakayama, H.; Raaschou, H.; Olsen, T. (1995). Recovery of walking function in stroke patients: the Copenhagen stroke study. *Archives of Physical Medicine and Rehabilitation*, Vol. 76, No. 1, (January 1995), pp. 76: 27-32, ISSN 0003-9993

MPD Costruzioni Meccaniche. (2010). Robot motor rehabilitation device, World Patent WO 2010/105773

Oppenheim, A.; Willsky, A.; Nawab, S. (1996). *Signals & Systems*, Prentice Hall, ISBN 0-13-814757-4, Upper Saddle River, New Jersey, USA

Simons, W. & Yang K. (1991). Differentiation of human motion data using combined spline and least squares concept. *Journal of Biomechanical Engineering*, Vol. 113, (August 1991), pp. 348-351, ISSN 0148-0731

Schmidt, H.; Hesse, S.; Bernhardt, R.; Krüger, J, HapticWalker-a novel haptic foot device., (2005) ACM Transactions on Applied Perception, Vol. 2, No. 2, (April 2005), pp. 166-180, ISSN 1544-3558

Veneman, J.; Kruidhof, R.; Hekman. E.; Ekkelenkamp, R.; Van Asseldonk, E.; van der Kooij, H. (2007) Design and evaluation of the LOPES exoskeleton robot for interactive gait rehabilitation. IEEE Transactions on Neural Systems and Rehabilitation Engineering, Vol. 15, No. 3 (September 2007), pp. 379-86, ISSN 1534-4320

Yoon, J.; Novandy, B.; Yoon C;, Park, K. (2010) A 6-DOF Gait Rehabilitation Robot with Upper and Lower-Limb Connections that Allows Walking Velocity Updates on Various Terrains. *IEEE Transaction on Mechatronics*, Vol. 15, No. 2, (April 2010), pp. 201-215, ISSN1083-4435

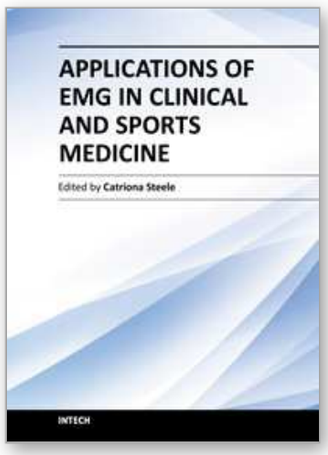

Applications of EMG in Clinical and Sports Medicine

Edited by Dr. Catriona Steele

ISBN 978-953-307-798-7
Hard cover, 396 pages
Publisher InTech
Published online 11, January, 2012
Published in print edition January, 2012

This second of two volumes on EMG (Electromyography) covers a wide range of clinical applications, as a complement to the methods discussed in volume 1. Topics range from gait and vibration analysis, through posture and falls prevention, to biofeedback in the treatment of neurologic swallowing impairment. The volume includes sections on back care, sports and performance medicine, gynecology/urology and orofacial function. Authors describe the procedures for their experimental studies with detailed and clear illustrations and references to the literature. The limitations of SEMG measures and methods for careful analysis are discussed. This broad compilation of articles discussing the use of EMG in both clinical and research applications demonstrates the utility of the method as a tool in a wide variety of disciplines and clinical fields.

How to reference

In order to correctly reference this scholarly work, feel free to copy and paste the following:

Christopher Tomelleri, Andreas Waldner and Stefan Hesse (2012). EMG Analysis Methods on Robotic Gait Machines, Applications of EMG in Clinical and Sports Medicine, Dr. Catriona Steele (Ed.), ISBN: 978-953-307-798-7, InTech, Available from: http://www.intechopen.com/books/applications-of-emg-in-clinical-and-sports-medicine/emg-analysis-methods-on-robotic-gait-machines

INTECH
open science | open minds

InTech Europe
University Campus STeP Ri
Slavka Krautzeka 83/A
51000 Rijeka, Croatia
Phone: +385 (51) 770 447
Fax: +385 (51) 686 166
www.intechopen.com

InTech China
Unit 405, Office Block, Hotel Equatorial Shanghai
No.65, Yan An Road (West), Shanghai, 200040, China
中国上海市延安西路65号上海国际贵都大饭店办公楼405单元
Phone: +86-21-62489820
Fax: +86-21-62489821

IntechOpen